Fluorinated hydrogenated amorphous silicon alloys. II. Electronic structure of pure and fluorinated silane chains

Savitri Agrawal and Bal K. Agrawal
Physics Department, Allahabad University, Allahabad 211002, India
(Received 4 May 1984; revised manuscript received 12 September 1984)

A theoretical study of the electronic structure of hydrogenated amorphous silicon alloys (a-Si:H) has been made after employing a cluster Bethe-lattice formalism. A number of silicon-fluorine-hydrogen configurations, e.g., simple units such as the SiH_n, SiF_nH_m ($m,n=1,2$, $m+n\leq 3$) and the chainlike configurations $(SiH)_n$, $(SiH_2)_n$, and $(SiFH)_2$ embedded in amorphous silicon, have been investigated using a realistic tight-binding Hamiltonian considering nearest-neighbor and next-nearest-neighbor interactions within the cluster. The local densities of states at H and Si atoms in alloys incorporating high H concentrations reveal structures in excellent agreement with the photoemission data. For low H concentration, a low-energy peak in the photoemission data can be understood in terms of the two adjacent interacting monohydrides. Thus, the occurrence of simple units and chainlike $(SiH)_n$ and $(SiH_2)_n$ configurations can explain most of the photoemission data in pure hydrogenated silicon samples very well. The same conclusion has recently been drawn after an analysis of infrared and Raman data by ourselves elsewhere. Furthermore, we predict the electronic spectra for the a-Si:F:H samples arising from the simple SiF_nH_m units and the $(SiFH)_n$ chainlike configurations. We observe that the locations of the peaks induced by F atoms remain undisturbed by the incorporation of H atoms. However, the positions of H-induced peaks are altered by the presence of the F atoms. Photoemission measurements on a-Si:F:H alloys need to be performed to detect the predicted electronic structure for a-Si:F:H alloys.

I. INTRODUCTION

Considerable interest has been shown recently in the study of the various properties of amorphous silicon (a-Si) alloys with incorporated hydrogen. It originates from the observation of Spear and Le Comber[1] that the amorphous hydrogenated silicon alloy (a-Si:H) can be doped substitutionally by phosphorous and boron impurities. A similar observation was made by Paul *et al.*[2] These studies, together with the good electronic properties of this material, made apparent the passivation of dangling bonds present in the pure a-Si. Recently, it has been shown[3] that the density of the electronic states in the middle of the gap is reduced through hydrogenation from $\sim 10^{20}$ cm^{-3} eV^{-1} to $\sim 5\times 10^{14}$ cm^{-3} eV^{-1}, and also leads to a sufficiently high carrier lifetime for improved efficiency of solar cells. Furthermore, hydrogenation widens the gap,[4-6] thus causing behavior as a wide-window-gap material.

The role of hydrogen in modifying the network of a-Si has been investigated by a number of experimental techniques such as infrared and Raman spectroscopy,[7,8] nuclear magnetic resonance,[9] small-angle x-ray scattering,[10] H implantation in crystalline silicon,[11] and neutron-scattering measurements.[12] We refer to reviews written by Spear,[11] Moustakas,[3] Fritzsche,[13] and Paul and Anderson[14] for the details of experimental work.

During the investigations of the structural, vibrational, electronic, and transport properties of a-Si:H, quite interesting observations were made.[15] The photoemission measurements by von Roedern *et al.*[16] and Smith and Strongin[17] have revealed states due to hydrogen well within the valence band. The photoconductivity data of Moustakes *et al.*[18] has suggested the formation of Si:H antibonding states in the conduction band. The holes have a much lower mobility compared to electrons, suggesting the presence of a high density of localized states near the valence-band edge. The other experimental facts are the presence of an optically induced spin signal, two peaks in the gap (as observed in field-effect measurements), and recession of the valence-band edge with increasing H concentration. In the photoemission spectra, high-temperature modifications associated with the structures identical to those observed in Si(111):H and Si(100):H have been reported. A shift in the photoconductivity edge with increasing H concentration has been seen, which indicates the occurrence of Si—H antibonding states near the bottom of the conduction band.

Furthermore, the amount of hydrogen present in the a-Si:H alloys is as large as 100 times the maximum number of dangling bonds. The excess hydrogen is assumed to enter in sites as "stress points," allowing for a greater flexibility in growing an amorphous network of undistorted Si tetrahedra of crystalline silicon.

In hydrogenated a-Si, Brodsky *et al.*[7] have suggested the occurrence of SiH, SiH_2, and SiH_3 configurations by analyzing their Raman and infrared data. However, others[8,9] have proposed the presence of a majority of H atoms as short $(SiH_2)_n$ chains only, and have found no need of SiH_3 complexes. The observation of two characteristic temperatures in H effusion experiments hints toward the occurrence of SiH and SiH_2 complexes. Freeman and Paul[6] and John *et al.*[19] also found evidence for SiH_2 units, but not for SiH_3 units.

A few theoretical attempts to understand the electronic properties of a-Si:H alloys have been made. Using a generalized cluster-Bethe-lattice method, Allan and Joannopoulos[15,20] identified the peaks in photoemission spectra as signatures of the nearest-neighbor Si-H interactions and discussed the occurrence of states in the gap due to various defects. However, no comparison with the photoemission data was made by them for the alloys containing a high concentration of H atoms. Johnson *et al.*[21] made self-consistent-field $X\alpha$ scattered-wave (SCF $X\alpha$ SW) molecular-orbital calculations for the silane molecules and clusters. Electronic states for a series of realistic structural models were computed by Ching *et al.*[22] using an orthogonalized linear combination of atomic orbitals (OLCAO) method for a continuous-random-tetrahedral-network (CRTN) structural model of a-Si. They found a Si-H-H-Si model (a broken Si—Si bond with two H atoms inserted) in good agreement with several sets of experiments. Quite recently, calculations for a vacancy with four H atoms satisfying the dangling bonds have been performed by Divincenzo *et al.*[23] and by Papaconstantopoulos and Economou.[24] The former authors found the effect of compositional disorder as great as that of topological disorder. Barring the appearance of an extra peak in the low-energy region, the latter obtained an electron density in the valence band in agreement with the photoemission experiments, and also predicted the occurrence of antibonding Si-H states in the conduction band.

Guttman and Fong[25] have used periodic models for a self-consistent pseudopotential calculation and have seen some bonding states lying just below the bottom of the valence band which originate from the three-center bond. For a discussion of the theory of the electronic structure of a-Si:H, we refer to a recent review article.[26]

Recently, we[27–30] have been engaged in a detailed and comprehensive study of the vibrational and electronic excitations in hydrogenated fluorinated amorphous silicon alloys using a cluster-Bethe-lattice method (CBLM). In a letter[27] we showed that most of the infrared data of a-Si:F:H alloys can be understood in terms of the simple five-atom complexes containing F and H atoms. Subsequently, we discussed the effect of the chainlike $(SiF)_n$ and $(SiF_2)_n$ configurations on the infrared data, and the electronic[28] and vibrational[29] excitations of the a-Si, and found that some of the peaks seen in the infrared data which remained unexplained on the basis of simple units may originate due to these chains. In addition, the photoemission data of these alloys have been explained[28] by a tight-binding Hamiltonian in the CBLM (hereafter, Ref. 28 will be referred to as paper I). Similarly, we have shown[30] that, in pure hydrogenated and fluorinated alloys, peaks detected in the infrared and Raman data of heavily doped samples can be understood on the basis of the occurrence of the simple SiH_n units and/or their chainlike $(SiH)_n$, $(SiH_2)_n$, and $(SiFH)_n$ configurations.

In the present paper we pursue our study of the electronic structure of the amorphous silicon containing SiH_n $(n=1,3)$, SiFH, SiF_2H, and $SiFH_2$ units, and also the chainlike configurations $(SiH)_n$, $(SiH_2)_n$, and $(SiFH)_n$. The predicted structure is compatible with the available photoemission data.

We find that the photoemission data can be understood very well in terms of the above-mentioned units. A peak observed in the low-energy region of the photoemission data of an alloy incorporating a low concentration of H atoms can be explained on the basis of the two interacting monohydrides lying on the nearest-neighbor sites, an observation also made by Allan and Joannopoulos.[15] In Sec. II we give a brief account of the cluster-Bethe-lattice formalism. Section III contains the results for the various complexes attached to the silicon matrix. A comparison with the photoemission data is also given there. Excellent agreement between the theory and experiment is seen. In Sec. III B, we present the results for the electronic density of states for the F and H mixed, SiFH, SiF_2H, and $SiFH_2$ complexes. The results for the fluorosilane $(SiFH)_2$ chainlike configuration in the trans configuration are also included there. The main conclusions are contained in Sec. IV.

II. THEORY

First, we performed a molecular-orbital calculation for the various isolated silicon-hydrogen configurations $Si_{5-m}H_m$ for $m=1$—4. We consider the nearest-neighbor and second-neighbor Si-H and H-H interactions. The electrons of each atom of Si are described by one s orbital and three p orbitals (p_x,p_y,p_z), and, for the H atom, the s orbital only. We need to know the following six interaction integrals for each Si—Si bond:

$$\begin{aligned} &E_s=\langle s\,|\,\underline{H}\,|\,s\rangle,\quad X=\langle s\,|\,\underline{H}\,|\,p'\rangle\ , \\ &E_p=\langle p\,|\,\underline{H}\,|\,p\rangle,\quad V=\langle p_x\,|\,\underline{H}\,|\,p_x'\rangle\ , \\ &U=\langle s\,|\,\underline{H}\,|\,s'\rangle,\quad T=\langle p_x\,|\,\underline{H}\,|\,p_y'\rangle\ . \end{aligned} \tag{1}$$

Here the primes specify the atomic orbitals lying on the neighboring site of the reference atom.

For the Si—H bond, we need to know the interaction integrals U and X only. Similarly, for the H—H bond one should determine the interaction integral U only.

The set (E_s',E_p') denotes the atomic energies of the Si atom, and E_s denotes the atomic energy of the H atom. The set (U',V',T',X') denotes the nearest-neighbor interactions for the Si—Si bond, and (U,X) that for the Si—H bond. For the second-neighbor interactions, the parameters are (U''',X''') for the H—Si bond and U'' for the H—H bond.

A group-theoretical analysis was made to block-diagonalize the Hamiltonian matrix for the various units. The various symmetry coordinates, i.e., the coefficients of the linearized combinations of the atomic orbitals lying at the various atoms in the interaction space, have been given elsewhere.[31]

The Bethe lattice is an infinite network of atoms with the correct coordination devoid of any ring structure. The elementary excitations of a Bethe lattice show a smooth and featureless density of states, and can provide a natural background upon which the characteristic properties of the cluster can be studied. In a cluster-Bethe-lattice calculation, the dangling bonds of the surface atoms are con-

nected to a Bethe lattice. In this method, one thus treats a part of an infinitely connected network of atoms exactly as a cluster, and represents the effect of the environment by a Bethe lattice.

For a system containing a number of atoms, one may define a Green's function in a position representation by

$$\underline{G}=(E\underline{I}-\underline{H})^{-1}\ , \tag{2}$$

where $\underline{I}$ is the unit matrix, E is the energy of the elementary excitation, and $\underline{H}$ is the Hamiltonian of the system. We may split the Hamiltonian as

$$\underline{H}=\underline{H}^0+\underline{V}\ , \tag{3}$$

where $\underline{H}^0$ is the diagonal part containing the self-site matrix elements; $\underline{V}$ is the nondiagonal part containing the matrix element representative of the various interactions between the different atoms of the system.

One may rewrite Eq. (2) as a Dyson equation,

$$(E\underline{I}-\underline{H}^0)\underline{G}=\underline{I}+\underline{V}\underline{G}\ . \tag{4}$$

The matrix elements of the above equation may be written explicitly as

$$E\langle i\mid\underline{G}\mid j\rangle=\underline{I}_{ij}+\sum_k\langle i\mid\underline{V}\mid k\rangle\langle k\mid\underline{G}\mid j\rangle\ . \tag{5}$$

The density of states at site i is determined by the imaginary part of the trace of the local Green's function as

$$N_i(E)=-\frac{1}{\pi}\,\mathrm{Im\,Tr}[\underline{G}_{ii}(E)]\ ,$$

with

$$\underline{G}_{ii}(E)=\langle i\mid\underline{G}\mid i\rangle\ . \tag{6}$$

The characteristics of the Bethe lattice can be exploited for the reduction of the infinite set of coupled equations (5) to a finite set by employing the effective fields or transfer matrices.[32] One represents the localized atomic orbitals by a dot. In the Bethe lattice possessing no rings, every dot can be transformed to another dot by a fixed set of transformations. Furthermore, the different dots are connected to each other by one self-avoiding path. As a consequence, the Green's function between two distant neighbors (i,k) is related to that between two nearer ones (i,j) by

$$\underline{G}_{ki}=\underline{t}_{kj}\underline{G}_{ji}\ . \tag{7}$$

Here, $\underline{t}_{kj}$ is the transfer matrix at site j in the direction of k.

The self-site Green's function may then be expressed as

$$\underline{G}_{ii}=(E\underline{I}-\underline{H}^0_{ii}-\underline{F})^{-1}\ ,$$

with

$$\underline{F}=\sum_j\underline{V}_{ij}\underline{t}_{ji}\ . \tag{8}$$

For details, we refer to paper I (Ref. 28).

TABLE I. Atomic-orbital energies for the free molecules (in eV). The energies have been measured with respect to the vacuum.

Orbitals	Si	H
E_p	−6.52	
E_s	−12.77	−11.10

III. CALCULATIONS AND RESULTS

A. Pure hydrogenated *a*-Si alloys

1. Evaluation of the parameters

Before making any calculation for the various units, we need to know the interaction parameters for the several Si—Si, Si—H, H—H, etc. bonds, along with the self-site energies. The atomic-orbital energies used for Si and H atoms are shown in Table I. The value for the s orbital of H is in accordance with that of Pandey.[33] (However, the present given value is measured with respect to the vacuum, in contrast to that of Pandey, −3.38 eV, which is measured with respect to the top of the valence band.)

The interaction integrals for the Si—H bond are determined after performing a molecular-orbital calculation for the intensively experimentally studied[34–36] stable molecule SiH_4. The experimental values for the SiH_4 molecule are taken as input. The calculated values for the various molecular orbitals are compared with the experimental values in Table II, and the determined values of the parameters for the first- and second-neighbor interactions are presented in Table III. The values for the Si—Si have already been determined in paper I. For the second-neighbor interaction U for the Si—H bond, an average of those for the Si—Si and H—H bonds has been taken.

These parameters are then tested by evaluating the energy values for the stable molecule Si_2H_6. The calculated values for the various molecular orbitals, along with their constituency, are compared with the available experimental values[33] in Table IV. A very good agreement is seen.

We now obtain the molecular-orbital energies for the various $Si_{5-m}H_m$ $(m=1,3)$ units. In the Si_4H unit the H-induced s-orbital bonding state appears at −13.25 eV, which, when measured with respect to the top of the valence band of the silicon matrix (a shift of −7.72 eV), would be −5.5 eV. In the Si_3H_2 group the H-induced state occurs at −12.77 (−5.0) eV, and in the Si_2H_3 group it occurs at −12.74 (−5.0) and −9.35 (−1.6) eV, respectively.

TABLE II. Energies of the various molecular orbitals for the SiH_4 molecule (in eV) (AO denotes atomic orbital).

Molecular orbital	Eigenvalues Calculated	Eigenvalues Experimental	Main AO components
A_1	−19.22	−18.20[a]	Si 3s, H 1s
F_2	−12.71	−12.70[a]	H 1s, Si 3p
F_2	−5.42	−5.40[b]	Si 3p, H 1s
A_1	−4.12	−4.10[c]	Si 3s, H 1s

[a]Reference 34.
[b]Reference 35.
[c]Reference 36.

TABLE III. Values of the first- and second-neighbor matrix elements for the different bonds (in eV).

Bond	U	X	V	T
		First-neighbor interactions		
Si—Si	−1.94	1.01	1.73	0.66
Si—H	−3.433	1.307		
		Second-neighbor interactions		
H—H	0.51			
H—Si	0.2505	0.00		

2. SiH_n units in the CBLM

In Fig. 1 we reproduce the valence-band photoemission spectra measured by von Roedern *et al.*[16] for the hydrogenated amorphous silicon samples prepared by different methods at different temperatures. It may be noted that the high-temperature samples, i.e., the glow-distance sample annealed at 350 °C [Fig. 1(a)] and the sputtered sample at 350 °C with hydrogen [Fig. 1(b)], show quite similar features in the photoemission cross section, i.e., four peaks in the spectra. The samples prepared at room temperature by glow discharge or sputtering [Figs. 1(c) and 1(d)] also reveal similar features (peaks A and B). However, the separation of peaks A and B is seen to be different.

The electronic density of states for the Bethe lattice simulating the amorphous silicon has been obtained in paper I. For completeness, we reproduce it in Fig. 2(a). The density is quite smooth and featureless, and arises mainly from the s orbitals in the low-energy region and from the p orbitals near the top of the valence band.

The electron density at the H atom and the averaged density over the five atoms in the cluster have been calculated and are presented in Figs. 2—4.

In the glow-discharge- or the sputter-produced a-Si:H films, which either have a high substrate temperature of 350 °C or are annealed at 350 °C, one finds a comparatively low concentration of H atoms. In all, there are four peaks (Fig. 1). The peak close to the top of the valence band is also seen in the spectrum of bulk silicon. Thus C, D, and E are the H-induced peaks. By comparing these spectra with the measurements performed on H-adsorbed Si(111) surfaces, one may interpret the appearance of peaks C and D as originating from the monohydrides (SiH units) lying on the next-nearest-neighbor Si sites.[26] In the following we first discuss the features in the spectra arising from an isolated SiH unit, and consider the interacting monohydrides in the next section.

For a SiH unit [Fig. 2(a)] in the silicon bulk, the s-like electronic density of states at the H atom reveals a broad peak at −4.0 eV, compared to a peak seen in the photoemission data for the sputter-produced sample at −5.2 eV. The H-induced s-electron-like density is also observed at Si* (a Si atom coupled to a H atom). In an attempt to match the theoretical and the experimental peaks [Fig. 2(b)], an arbitrary shift of 1.2 eV in the experimental peak toward the higher-energy side has been made. For a detailed discussion, we refer to Allan *et al.*[20]

There is a depletion of states near the top of the valence band, a result which is in agreement with the photoemis-

TABLE IV. Energy values for the various molecular orbitals for the Si_2H_6 molecule (in eV).

Molecular orbital	Eigenvalue Calculated	Eigenvalue Experimental[a]	Main AO components
A	−18.44		Si 3s, H 1s,
A	−17.19	−17.3	Si 3s, H 1s
E	−12.90	−13.3	H 1s, Si 3p
E	−12.57	−12.1	H 1s, Si 3p
A	−10.53	−10.7	Si 3p, H 1s, Si 3s
E	−6.31		Si 3p, H 1s
A	−5.39		Si 3s, H 1s, Si 3p
E	−4.49		Si 3p, H 1s,
A	−4.13		Si 3s, H 1s
A	−3.07		Si 3p, Si 3s

[a]Reference 36.

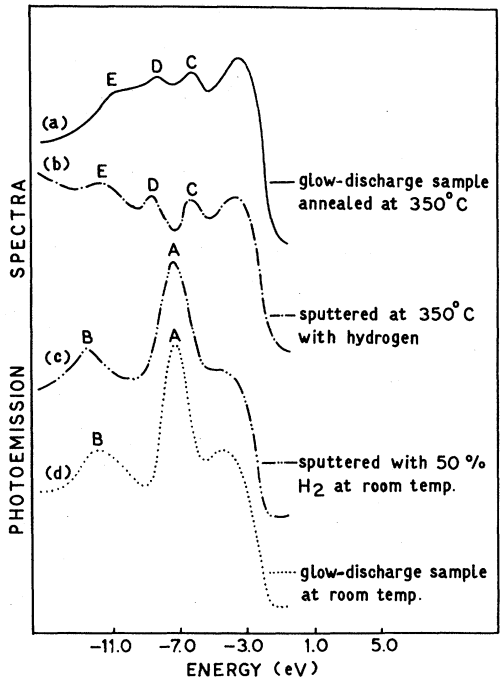

FIG. 1. Valence-band photoemission spectra of von Roedern *et al.* (Ref. 16) for the a-Si:H films prepared by different techniques: (a) glow-discharge-produced sample annealed at 350 °C; (b) sputter-produced sample at 350 °C with hydrogen; (c) a-Si sample sputtered with 50 vol % H_2 at room temperature; (d) glow-discharge-produced sample at room temperature.

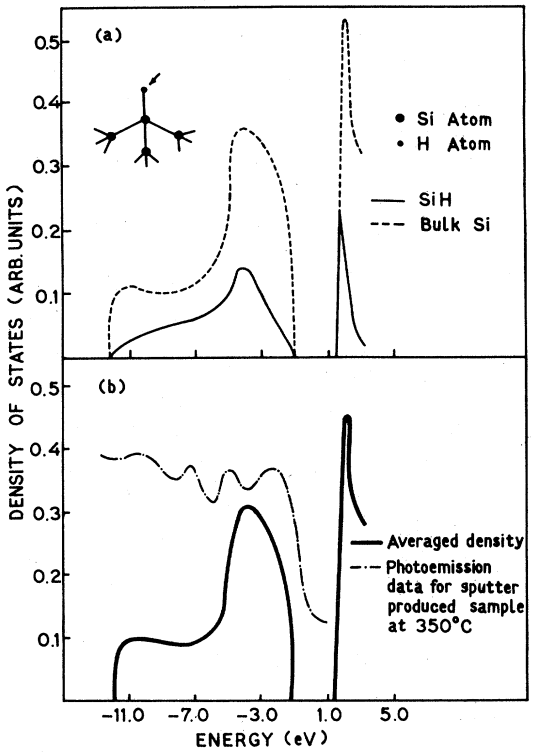

FIG. 2. (a) Electronic density of states for a bulk-silicon Bethe lattice and for SiH unit at H atom coupled to the Bethe lattice. (b) Comparison of the electronic density averaged over five atoms of the cluster Si_4H with the photoemission data for a sputter-produced a-Si:H sample at 350°C.

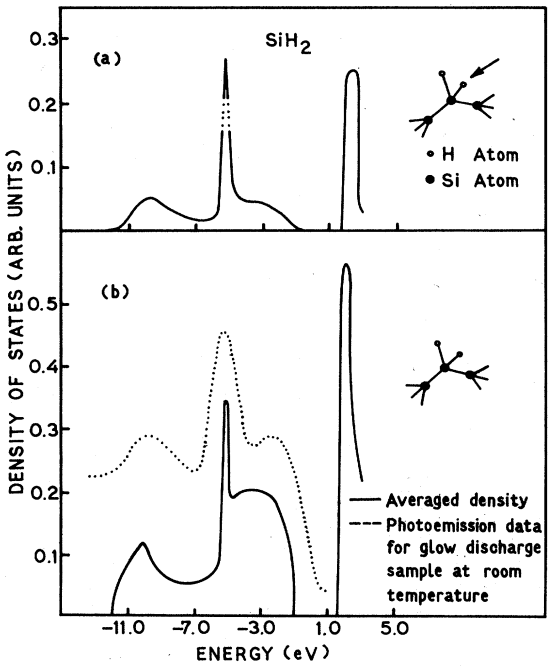

FIG. 3. Electronic density of states for SiH_2 unit (a) at H atom attached to the Bethe lattice, and (b) averaged density over five atoms of the cluster Si_3H_2 along with the photoemission data for a glow-discharge-produced sample at room temperature.

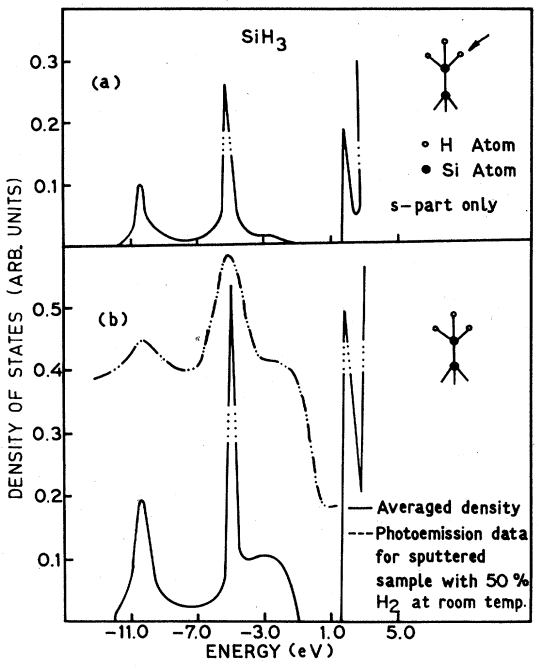

FIG. 4. The key is similar to Fig. 3, but for the SiH_3 unit. The photoemission spectra are for a silicon sample sputtered with 50 vol % H_2 at room temperature.

sion data. In addition, Si—H antibonding states appear at the bottom of the conduction band. These states would lead to a low conduction-band mobility, as has been seen in the photoconductivity experiments of Moustakas *et al.*[18] The two other peaks (D and E) in the low-energy region in the photoemission data do not appear in the calculated density. We will discuss the origin of this extra structure in the following section.

von Roedern *et al.*[16] have measured the variation of photoemission cross section with energy for the glow-discharge-produced, as well as for the sputter-produced, a-Si:H films at room temperature (see Fig. 1), where a large amount of hydrogen is incorporated into these samples. The incorporated hydrogen gives rise to two prominent peaks, denoted A and B. There are small but distinct differences between the films prepared by sputtering in an Ar/H_2 mixture and those prepared by the glow-discharge technique on room-temperature substrates [see Figs. 1(c) and 1(d)]. The separation between peaks A and B is (5.0 ± 0.2) eV in the case of sputtered film and (4.5 ± 0.2) eV in the case of glow-discharge film. We have conjectured that a decrease of the A-B splitting is associated with a shift from SiH_3 to $(SiH_2)_x$ bonding in the case of glow-discharge samples. We investigate the electronic structure originating from the various types of bondings in the heavily doped a-Si:H alloys, in order to shed light on this problem, in the following sections.

For the SiH_2 unit [Figs. 3(a) and 3(b)] in the silicon bulk, the s-like electronic density at the H atom [Fig. 3(a)] reveals two peaks, at -5.1 and -9.9 eV (a separation of 4.8 eV), having different strengths. The low-energy peak at -9.9 eV, having a comparatively smaller strength, originates from the s-like electrons of the silicon matrix.

The higher-energy peak at −5.1 eV, having greater strength, extends up to the Si* atom and is somewhat delocalized. A broad silicon p-like density has emerged near −3 eV in the theoretical curve. The electronic density at the H atom in the neighborhood of the top of the valence band is depleted further with an increase in the amount of the incorporated hydrogen, in agreement with the photoemission data. The number of Si—H antibonding states also increases.

For the SiH_3 unit (Fig. 4), similar to the SiH_2 unit, two H-induced peaks appear, at −5.1 and −10.3 eV, having a larger separation (of 5.2 eV) in the s-like electronic density at the H atom. Going from the SiH_2 to the SiH_3 configuration, the peak at −5.1 eV remains undisturbed. However, the peak lying in the low-energy region shifts by 0.4 eV. In addition, there is a further depletion of density at the top of the valence band, and an enhancement in the antibonding states at the bottom of the conduction band.

Upon comparing the present results with the photoemission data, we find that, as the calculated A-B splitting is smaller in the case of the SiH_2 unit compared to the SiH_3 unit, one can ascribe the structure (peaks A and B) seen in the glow-discharge sample at room temperature to the occurrence of the SiH_2 units. The large splitting seen in the sputter-produced sample with 50 vol% H_2 at room temperature may originate from the presence of SiH_3 units. The calculated shift of 0.4 eV in the A-B splittings for the SiH_2 and SiH_3 bondings is in good agreement with the measured shifts of 0.3—0.5 eV.

We have compared the calculated electron density for SiH_2 bonding with the photoemission spectra, for the glow-discharge sample at room temperature, in Fig. 3(b). In order to match the peaks, again a shift of the experimental curve by 1.2 eV has been made toward the higher-energy side. Very good agreement for the locations and strengths of the peaks between the averaged electron density and the photoemission spectra is seen. The calculated peaks at −5.1 and −9.9 eV are in close agreement with the experimental ones at −6.3 and −10.8 eV, respectively.

The calculated electron density for SiH_3 bonding has been compared with the photoemission spectra, for the hydrogenated a-Si film prepared by sputtering at room temperature, in Fig. 4(b). Good agreement is seen between the calculated peak positions at −6.3 and −11.3 eV and the photoemission-data peaks at −6.3 and −11.6 eV. Similar conclusions have also been drawn by Ching *et al.*[22] and by Allan and Joannopoulos.[26] It is to be noted that the measured photoemission spectra may not always mimic the electron density of states exactly. Matrix-element effects will appear in the photoemission spectra because of the variation of the photoemission cross section with energy, which has not been considered in the above discussion.

Thus we find good agreement between the theoretical results for SiH_2 and SiH_3 units with the photoemission data for the glow-discharge- and sputter-produced films, regarding the location of the peaks in the electronic density. However, a peak appearing in the low-energy region of the photoemission data for a low concentration of H atoms does not appear in the calculated density of a single SiH unit. This peak may arise either from the ring structure of the silicon network or from the interacting SiH units.[20] We investigate the latter possibility here. Allan *et al.*[15,20] have seen extra structure in electron density arising both from the rings in the silicon network and the interacting SiH units.

3. $(SiH)_n$ and $(SiH_2)_n$ chains

We next perform calculations for the $(SiH)_n$ and $(SiH_2)_n$ chains.

For the $(SiH)_2$ complex, i.e., two interacting monohydrides lying on the nearest-neighbor sites embedded in a-Si, the calculated electron density, as shown in Fig. 5, contains, in all, three peaks at the H and Si* atoms located at −10.6, −8.4, and −4.7 eV (see Table V). They are quite compatible with peaks E,D, and C seen in the photoemission data for the high-substrate-temperature, sputtered a-Si:H films at 350°C appearing at −10.8, −7.6, and −5.2 eV, respectively. The two Si-H low-energy peaks induced by H atoms are seen mainly at the Si* atom, whereas the high-energy peak appears both at the H and Si atoms and is somewhat delocalized. Allan *et al.*[20] have found the origin of the extra peaks in the rings of the bonds of the Si network also. We refer to their discussion. Combined ultraviolet and x-ray photoelectron spectroscopy (UPS and XPS) measurements on the same samples may be useful in discerning the two possible explanations. The x-ray scattering for the H atom has a low cross section.

A peak of the Si-H antibonding states appears in the band gap just below the bottom of the conduction band. The presence of antibonding states in the pseudogap has been established in a number of experimental measurements.[18]

For the two interacting SiH_2 units lying on the nearest-neighbor sites, i.e., $(SiH_2)_2$, the electron density shown in

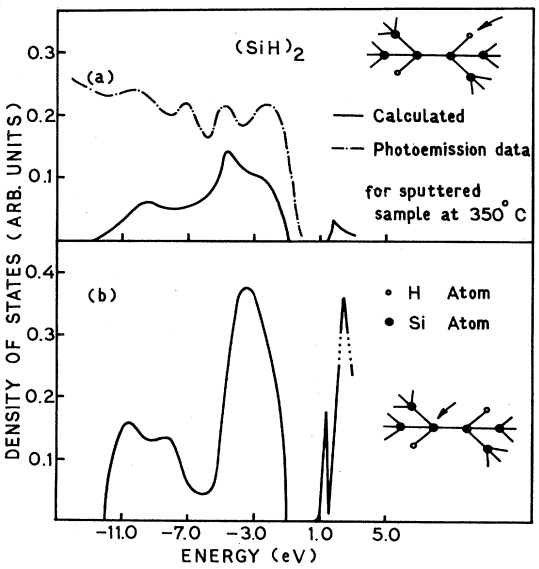

FIG. 5. Electronic density of states for two interacting monohydrides [$(SiH)_2$] with photoemission data for a sputter-produced sample at 350°C.

TABLE V. Comparison of the calculated peak positions for the $(SiH)_n$ units with the photoemission data in a-Si:H alloys, measured in eV.

Calculated peak position		
SiH	$(SiH)_2$	Photoemission data
	−10.6	−10.8
	−8.4	−7.6
−4.1	−4.7	−5.2

Fig. 6 reveals splitting of all the peaks seen earlier for a single SiH_2 unit. These states are quite delocalized since a quite appreciable density appears at the attached Si* atom. The energies of the split peaks are given in Table VI. The Si p-H s—like peak, at −3 eV, of the SiH_2 unit splits both at the Si and H atoms. Splittings of about 1.7 and 0.4 eV appear for the −9.9- and −5.1-eV, peaks, respectively. However, these splittings are not very large and lie well within the broad peaks of the photoemission data for the specimen sputtered with 50 vol% H_2, as has been shown in Fig. 6(a).

Upon increasing the size of the chain by adding one more SiH_2 unit, i.e., for $(SiH_2)_3$, further splittings of the peaks in the electron density take place (Fig. 7). The electron density at the exterior and interior H atoms are shown separately in Figs. 7(a) and 7(b), respectively. Similar to the $(SiH_2)_2$ complex, the high-energy peak shows splitting only at the H atom connected to the silicon network, i.e., the exterior one. Again, the total splittings in the three peaks are about −2.5, −0.4, and 0.8 eV, respectively, and are well contained in the three broad peaks of the photoemission data for the sputtered sample. A large decrease in the number of s-like states at the interior H atoms takes place at the top of the valence band, leading to a larger band gap, as has been seen experimentally.

For a longer silane-like chain of four SiH_2 units, i.e., for a $(SiH_2)_4$ complex embedded in the a-Si, a spikier structure appears in the electron density, both at the exterior H atom [Fig. 8(a)] and the interior H atom [Fig. 8(b)]. However, the smoothened density is again very compatible with the photoemission data for the sputtered sample.

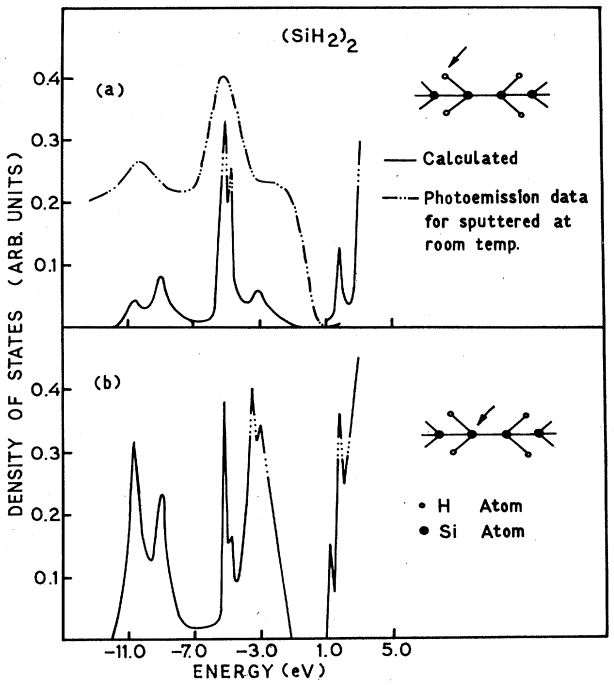

FIG. 6. Electronic density of states for two interacting dihydrides $[(SiH_2)_2]$ with photoemission data for a sample prepared by sputtering with H at room temperature.

The splittings increase slightly (Table VI), and the sharp peaks in the local electron density of H atoms show a molecular-like behavior, corresponding to SiH_2 units. The influence of the silicon matrix starts disappearing at the interior H atoms, whereas more reduction in electron density takes place at the top of the valence band, opening a wider band gap in a-Si:H alloys.

4. *Discussion*

In another paper,[30] we studied the vibrational excitations of the simple SiH_n units and those of their chainlike configurations, and compared the results with the available infrared and Raman data of the hydrogenated alloys. It was observed that most of the experimental data can be

TABLE VI. Comparison of the calculated peak positions for the $(SiH_2)_n$ units with the photoemission data in a-Si:H alloys, measured in eV.

		Calculated peak positions for $(SiH_2)_3$ at		$(SiH_2)_4$ at		
SiH_2	$(SiH_2)_2$	Si	H	Si	H	Photoemission data
		−10.65	−10.7	−10.8	−10.8	−11.3
	−10.65					
−9.9		−9.75	−9.7	−9.95	−9.95	
	−8.95	−8.8	−8.8	−9.2	−9.2	
				−8.25		
−5.1	−5.2	−5.0	−5.0	−5.2	−5.2	−6.3
	−4.8	−4.8	−4.8	−4.8	−4.8	
−3.0	−3.2	−3.6	−3.2	−3.6	−3.6	
		−3.0	−2.6	−2.6	−2.8	

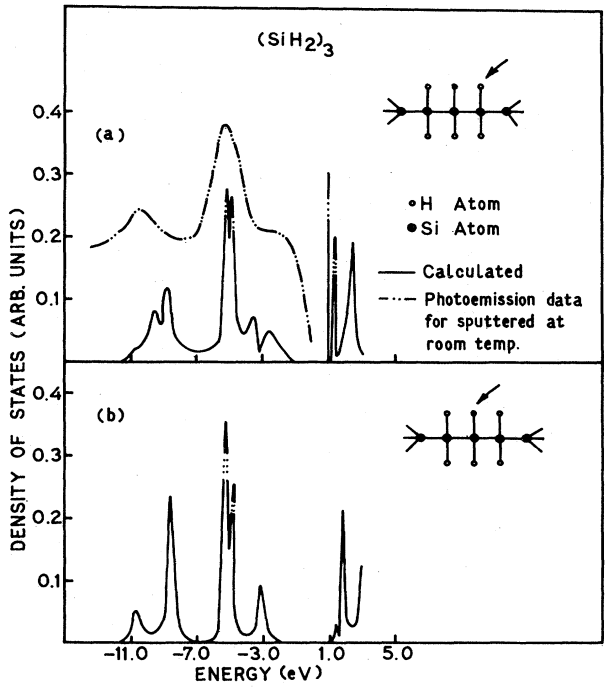

FIG. 7. They key is similar to Fig. 6, but for three interacting dihydrides [$(SiH_2)_3$].

well understood on the basis of the simple SiH_n ($n=1,3$) units. However, some of the unexplained observed peaks could be accounted for only by the presence of the interacting $(SiH)_2$ and $(SiH_2)_n$ units. The electronic structure discussed in the present paper also supports the same

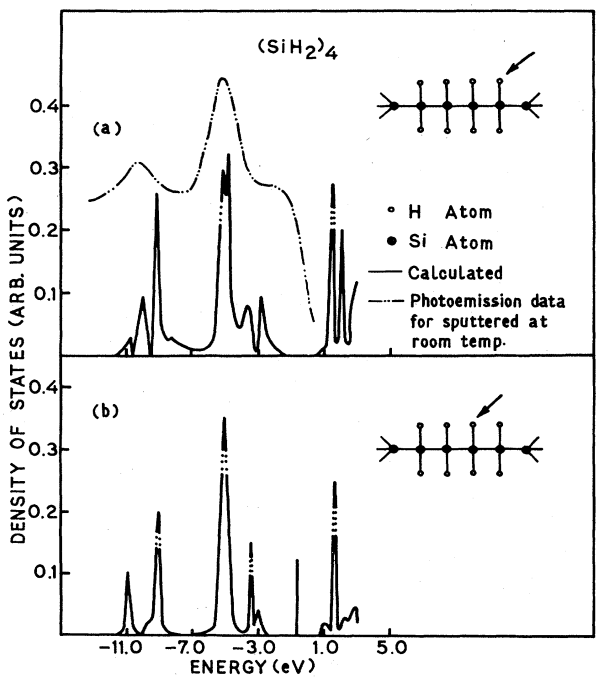

FIG. 8. The key is similar to Fig. 6, but for four interacting dihydrides [$(SiH_2)_4$].

proposition. The photoemission data can be very well understood on the basis of the assumed complexes. The photoemission data for the heavily hydrogen-doped silicon can be explained on the basis of the isolated dihydride and trihydride units. The splitting of the peaks of a SiH_2 unit arising from the interaction of these units lying on the neighboring sites is small, and is well contained within the broad experimental peaks. The photoemission data for a lightly doped sample can be understood in terms of the interacting monohydrides.

B. Fluorinated hydrogenated *a*-Si alloys

1. SiF_nH_m ($n,m=1,2$, $n+m\leq 3$) complexes

Carrying over the values of the interaction parameters for the Si—H and Si—F bonds from the corresponding pure hydrogenated and fluorinated[28] silicon alloys, we have performed calculations for the electron density for the SiFH, $SiFH_2$, and SiF_2H units coupled to the Bethe lattice for amorphous silicon. For complexes containing one F atom similar to a pure *a*-Si:F alloy, the *s*- and *p*-orbital energies for the F atom have been shifted by 1.8 eV towards the higher-energy side, and that for the complex containing two F atoms by 0.9 eV towards the higher-energy side. However, no shift in energy has been made for the *s* orbital of H atoms in all the H and F mixed configurations (see Table VII).

(a) SiFH unit. The local electron density for the SiFH unit coupled to amorphous silicon at the H, F, and Si

TABLE VII. Calculated peak positions for the different Si:F:H units (in eV). The atom activating the peak is indicated in parentheses.

Configurations	at H	at F	at Si
SiFH	−11.55	−11.6 (F)	−11.6
	−8.85	−8.85 (F)	−8.85
	−6.2 (H)	−6.3	−6.3
	−3.2 (H)	−2.3	−1.9 (Si)
SiF_2H	−12.6	−12.6 (F)	−12.6
	−10.3	−10.3 (F)	−10.3
		−9.65 (F)	−9.65
		−8.65 (F)	
		−8.35 (F)	−8.35
	−5.4 (H)	−5.4	−5.4
	−1.8	−1.6	−1.6 (Si)
$SiFH_2$	−11.65	−11.65 (F)	−11.65
	−8.85	−8.85 (F)	−8.85
	−6.8 (H)	−6.8	−6.8
	−4.6 (H)	−4.6	−4.6
	−2.4	−2.1	−1.9 (Si)
$(SiFH)_2$	−12.05	−12.05 (F)	−12.05
	−10.8	−10.8 (F)	−10.85
	−8.9	−8.9 (F)	−8.9
	−8.55	−8.55 (F)	−8.55
	−6.6 (H)	−6.6	−6.6
	−5.6 (H)	−5.6	−5.6
	−2.6	−2.6	
		−1.6	−1.6 (Si)

atoms is depicted in Figs. 9(a), 9(b), and 9(c), respectively. Now the H-induced peak appears at -6.3 eV, in contrast to the peak at -4.0 eV in the pure hydrogenated silicon alloy seen in Sec. III A2. Thus, one notes a shift in the H s peak toward the low-energy side. On the other hand, the two p-like F-induced peaks appearing here at -8.9 and -11.6 eV, respectively, remain almost undisturbed by the incorporation of H atoms. The corresponding peaks in pure fluorinated alloy appear at -8.9 and -11.2 eV, respectively.

The H atom picks up extra electron states at the location of the two peaks induced by the F atom and vice versa. These states are thus somewhat delocalized and extend up to at least the second-neighbor atoms. The authors are not aware of any experimental measurements mimicking the electron density of states such as the photoemission experiments.

(b) SiF_2H unit. For the SiF_2H unit, the localized density of states at the H, F, and Si atoms of the cluster are presented in Figs. 10(a), 10(b), and 10(c), respectively. The H s peak now appears at -5.4 eV, again showing a shift towards the low-energy side, as compared to its location seen for the SiH unit in a pure a-Si:H alloy. On the other hand, all the p-like F-induced peaks seen earlier to appear for the SiF_2 unit in the pure a-Si:F alloys are present in the electron density of the SiF_2H unit exactly at the same locations, i.e., they now occur at -12.6, -10.3, -9.65, -8.65, and -8.35 eV, respectively.

As the H atom picks up electron density at the two F-induced peaks at -12.6 and -10.3 eV only, these resonance states are somewhat delocalized, in contrast to the other remaining F-induced states, which are quite localized. In addition, the F atoms also pick up some H s resonance states which are also comparatively delocalized. The peaked densities at -8.35 and -8.65 eV are very localized, as these states are not seen even at the nearest-neighbor Si atom. Again, no photoemission data for a-Si:H alloys are available for comparison with the predicted structure.

(c) $SiFH_2$ unit. The localized electron density for the FH_2 unit at H, F, and Si atoms is depicted in Figs. 11(a), 11(b), and 11(c), respectively. The H-induced peaks now appear at -4.6 and -6.8 eV, in contrast to their locations in pure a-Si:H alloys, where they are seen at -5.1 and -9.9 eV, respectively. Hence, the incorporation of F atoms shifts the H-induced peaks towards the higher-energy side by different magnitudes. This behavior is totally different from what has been seen above in the fluorinated alloys containing one H atom in the configurations in which a shift of the H-induced peak towards the low-energy side was found.

On the other hand, the F-induced peaks appearing at -8.85 and -11.65 eV are seen to occur almost exactly at their locations found in the pure a-Si:F alloys. Thus, the incorporation of an H atom does not influence the F-induced peak positions.

All the dopant-activated peaks are somewhat delocalized as appreciable densities of states due to them are ob-

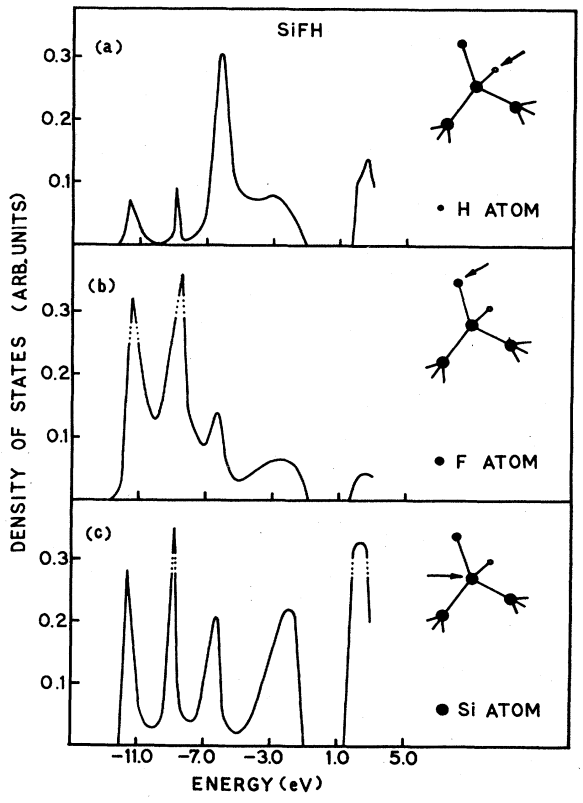

FIG. 9. Electronic density of states for SiFH configuration.

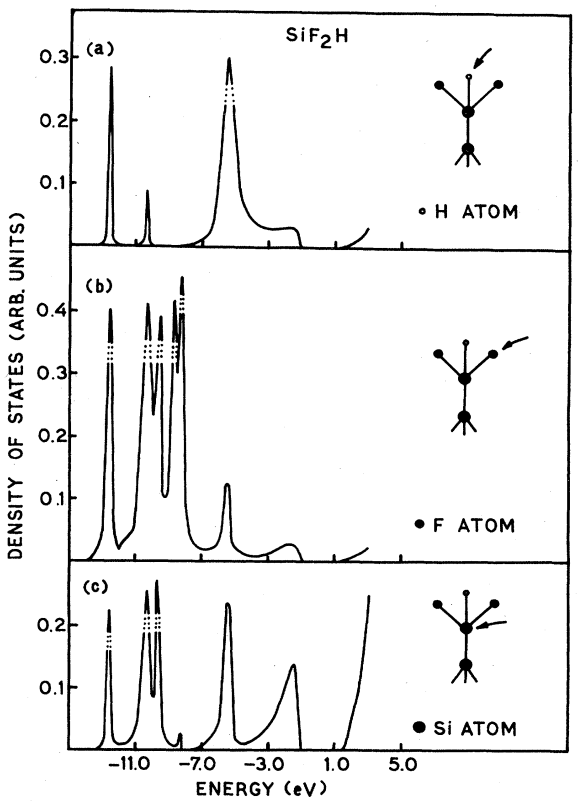

FIG. 10. Electronic density of states for the SiF_2H unit.

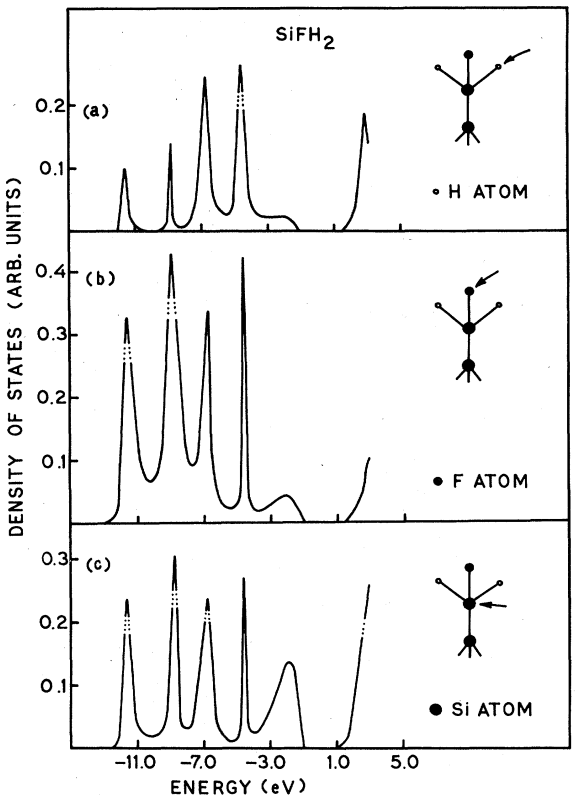

FIG. 11. Electronic density of states for the $SiFH_2$ unit.

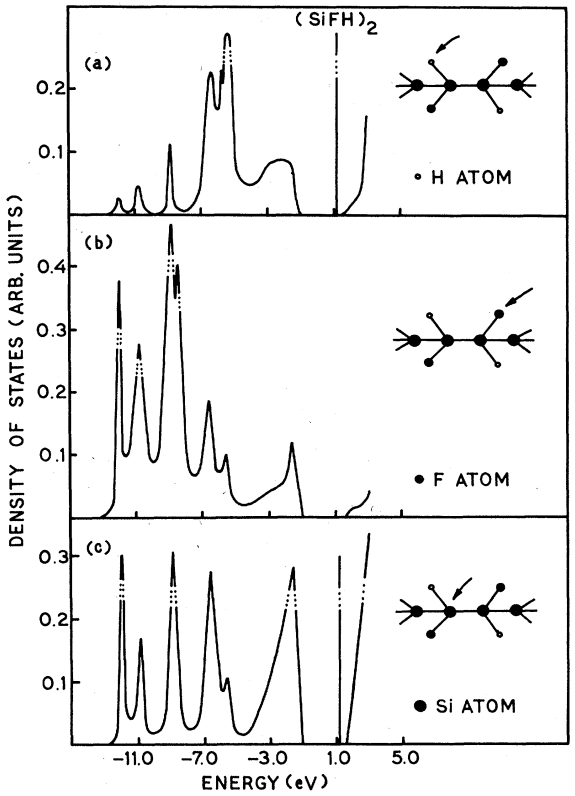

FIG. 12. Electronic density of states for two interacting SiFH units.

served at the coupled Si* atom. All the above results for SiF_mH_n complexes are in qualitative agreement with the conclusions of Ching,[37] barring a few differences. For example, Ching has found an extra peak in the low-energy region, -17 to -20 eV, for SiFH, SiFFH, and SiFHH complexes, which is not seen in the present results.

2. $(SiFH)_n$ complexes

We now turn toward the study of the two interacting SiFH units lying on the nearest-neighbor sites, for which the density at different atoms has been presented in Fig. 12. All the F- and H-induced peaks seen in the single SiFH unit show splittings of about 1 eV. The H-atom peaks appear at -5.6 and -6.6 eV, showing a splitting of 1 eV. The F-atom-induced peaks appear at $[-8.55, -8.9]$ eV and at $[-10.8, -12.05]$ eV, with splittings of 0.45 and 1.25 eV, respectively.

Furthermore electron density appears at the H atom in the gap just below the bottom of the conduction band. A similar density was seen earlier for the two interacting SiH units (see Fig. 5). These antibonding states have been detected in a number of measurements made on a-Si:H alloys.

Calculations have also been extended to the interacting three and four SiFH units, i.e., to $(SiFH)_3$ and $(SiFH)_4$ chains attached to the Bethe lattice. The F- and H-induced states split further, and the number of the peaks increases with the number of SiFH units. However, the magnitudes of these splittings are not very large.

IV. MAIN CONCLUSIONS

The present CBL calculation has been seen to be able to very successfully explain the photoemission data available for pure hydrogenated silicon alloys. The structures in the simple SiH_n units give rise to electronic densities of states which have been detected in the experimental measurements. However, the two interacting monohydrides SiH lying on the nearest-neighbor sites give rise to three peaks in the electronic density, in agreement with the photoemission data for an alloy containing comparatively a low concentration of H atoms.

Two other theoretical observations, i.e., the depletion of electron density near the top of the valence band and an enhancement in the antibonding states just below the bottom of the conduction band have been seen in the experimental measurement.

Extra structure in the electron density originates from the interacting SiH_2 units, i.e., in the silane-like $(SiH_2)_n$-chain configurations. However, this structure, combined with the effects of the quantitative disorder present in an amorphous phase, may not reveal itself in the experiments. A number of peaks in the phonon density of states having their origin in these chainlike configurations have been predicted by our group elsewhere, and they have been detected in infrared measurements made on a-Si:H alloys.

The electron density for the SiFH, SiF_2H, and $SiFH_2$ units and the $(SiFH)_n$ chains have shown all the dopant-induced peaks. The locations of all the F-induced peaks remain almost unaffected by the presence of H atoms in

these complexes. On the other hand, the H-induced peaks change their positions in the bulk-silicon electron density by the incorporation of the F atoms. Splittings in the F- and H-induced peaks appear in the interacting SiFH units. However, these splittings are not very large.

ACKNOWLEDGMENTS

We are grateful to the Department of Science and Technology and the University Grants Commission, New Delhi, for financial assistance.

[1]W. E. Spear and P. G. Le Comber, Solid State Commun. **17**, 1193 (1975).
[2]W. Paul, A. J. Lewis, G. A. N. Connell, and T. D. Moustakas, Solid State Commun. **20**, 969 (1976).
[3]T. D. Moustakas, J. Electron Mater **8**, 391 (1979).
[4]E. C. Freeman and W. Paul, Phys. Rev. B **20**, 716 (1979).
[5]G. D. Cooly, C. R. Wronski, B. Abeles, R. B. Stephens, and B. Brooks, Sol. Cells **2**, 227 (1980).
[6]N. B. Goodman, H. Friyzsche, and H. Ozaki, J. Non-Cryst. Solids **35—36**, 599 (1980).
[7]M. H. Brodsky, M. Cardona, and J. J. Cumo, Phys. Rev. B **16**, 3556 (1977).
[8]J. C. Knights, G. Lucovsky, and R. J. Nemanich, Philos. Mag. B **37**, 467 (1978).
[9]W. E. Carlos and P. C. Taylor, Phys. Rev. Lett. **45**, 358 (1980).
[10]P. D. Antonio and J. H. Kannert, Phys. Rev. Lett. **43**, 1161 (1979).
[11]W. E. Spear, Adv. Phys. **26**, 811 (1977).
[12]T. A. Postal, C. M. Falco, R. T. Kampwirth, I. K. Schullar, and W. B. Yelon, Phys. Rev. Lett. **45**, 648 (1980).
[13]H. Fritzsche, Sol. Energy Mater. **3**, 447 (1980).
[14]W. Paul and D. A. Anderson, Sol. Energy Mater. **5**, 229 (1981).
[15]D. C. Allan and J. D. Joannopoulos, Phys. Rev. Lett. **44**, 43 (1980).
[16]B. von Roedern, L. Ley, and M. Cardona, Phys. Rev. Lett. **39**, 1576 (1977); B. von Roedern, L. Ley, M. Cardona, and F. W. Smith, Philos. Mag. B **40**, 433 (1979).
[17]R. J. Smith and M. Strongin, Phys. Rev. B **24**, 5863 (1981).
[18]T. D. Moustakas, D. A. Anderson, and W. Paul, Solid State Commun. **23**, 155 (1977).
[19]P. John, I. M. Odel, J. K. Thomas, and J. I. B. Wilson, J. Phys. (Paris) Collq. Suppl. 10, **42**, (1981).
[20]D. C. Allan, J. D. Joannopoulos, and W. B. Pollard, Phys. Rev. B **25**, 1065 (1982).
[21]K. H. Johnson, H. J. Kolari, J. P. de Neufville, and D. L. Morel, Phys. Rev. B **21**, 643 (1980).
[22]W. Y. Ching, D. J. Lam, and C. C. Lin, Phys. Rev. Lett. **42**, 805 (1979); Phys. Rev. B **21**, 2378 (1980); L. Guttman, W. Y. Ching, and J. Rath, Phys. Rev. Lett. **44**, 2513 (1980).
[23]D. P. Divincenzo, J. Bernholc, M. H. Brodsky, N. Lipari, and S. T. Pantelides, in *Tetrahedrally Bonded Amorphous Semiconductors (Carefree, Arizona)* a Topical Conference on Tetrahedrally Bonded Amorphous Semiconductors, edited by R. A. Street, D. K. Biegelson, and J. C. Knights (AIP, New York, 1981), p. 156 (AIP Conf. Proc. No. 73); D. P. DiVincenzo, J. Bernholc, and M. H. Brodsky, Phys. Rev. B **28**, 3246 (1983).
[24]D. A. Papaconstantopoulos and E. N. Economou, Phys. Rev. B **24**, 7233 (1981).
[25]L. Guttman and C. Y. Fong, Phys. Rev. B **26**, 6756 (1982).
[26]J. D. Joannopoulos, *The Physics of Hydrogenated Amorphous Silicon II,* Vol. 56 of *Topics in Applied Physics* (Springer, New York, 1984).
[27]Bal K. Agrawal, Phys. Rev. Lett. **46**, 774 (1981).
[28]Bal K. Agrawal and Savitri Agrawal, Phys. Rev. B **29**, 6870 (1984).
[29]Bal K. Agrawal and B. K. Ghosh (unpublished).
[30]B. K. Ghosh and Bal K. Agrawal (unpublished).
[31]Bal K. Agrawal and Savitri Agrawal, DST Project Report No. 2, Allahabad University, 1985 (unpublished).
[32]J. D. Joannopoulos, Phys. Rev. B **16**, 2764 (1977).
[33]K. C. Pandey, Phys. Rev. B **14**, 1557 (1976).
[34]M. L. Sink and G. E. Juras, Chem. Phys. Lett. **20**, 474 (1973).
[35]R. G. Cavell, S. P. Kowalozyk, L. Ley, R. A. Pollack, B. Mills, D. A. Shirley, and W. Perry, Phys. Rev. B **7**, 5313 (1973).
[36]A. W. Potts and W. C. Price, Proc. R. Soc. London, Ser. A **326**, 165 (1972).
[37]W. Y. Ching, J. Non-Cryst. Solids **35—36**, 61 (1980).